KAM torus frequency generation from two line element sets

Gregory R. Frey, Capt, USAF
Air Force Institute of Technology
Dr. William E. Wiesel
Air Force Institute of Technology

ABSTRACT

The Kolmogorov Arnold and Moser (KAM) theorem states that a lightly perturbed Hamiltonian system will have solutions which lie on a torus. Earlier work by the second author has shown that most Earth satellite orbits perturbed by the geopotential lie on KAM tori. The problem then arises as to how to convert the current satellite tracking orbits to KAM tori. A KAM torus is characterized by three frequencies and three phase angles. The frequencies are essentially the rates of change of the mean anomaly, the longitude of the ascending node, and the argument of perigee. In this paper we explore the determination of these three rates from the fitting of SGP4 two line element sets (TLEs), and then constructing KAM tori with the specified frequencies. The success of this process, and an idea of the residual errors, can then be obtained by comparing the SGP4 predictions with the KAM torus predictions. Second order polynomials are fit to data from TLEs over 18 months using a least squares technique. The first order coefficients are used as the torus basis frequencies while the second order terms are used to account for perturbations to the satellite's orbit such as air drag. Four cases are attempted using the Hubble Space Telescope and three rocket bodies as test subjects. A KAM torus with the desired basis frequencies is constructed and used to predict satellite position. For the final test case, this shows an oscillatory error with an amplitude of less than 80 km over a period of almost two years. The authors speculate that this is caused by periodic lunar and solar perturbations, masked in the SGP4 fits by frequent updates.

1. MOTIVATION

Current methods of orbit propagation using a general perturbations technique such as the SGP4 model can only accurately predict a satellite's position for a few days before an update is necessary. In order to obtain the information necessary to update the model, a series of observations made with radar or electro-optical sensors is necessary. If more accurate or long-term predictions are needed, for collision avoidance for example, numerical integration is used. While advances in computational technology have greatly reduced the time necessary to perform these integrations, they still take hours to complete. In addition, to predict position one week in advance for instance, the orbit must be integrated through all of the intermediate time steps to produce the one needed predicted location. A new method with comparable accuracy and less computational and observational cost would be beneficial.

2. BACKGROUND

Kolmogorov, Arnold, and Moser Theorem, or KAM Theorem, was originally developed in the 1950s as an attempt to solve the classical three-body problem. In words, KAM theorem states that for an integrable system in which the momenta and forces are invariant – that is, a Hamiltonian system – subject to small smooth perturbations from conservative forces, many solutions for the unperturbed system are also solutions to the perturbed system with small changes. The perturbed system contains one or more action-angle variables such that the Hamiltonian can be written as

$$\mathrm{H}(J,\omega) = h(J) + \epsilon f(J,\omega) \tag{1}$$

Where J and ω are the action-angle variables, h is the unperturbed Hamiltonian, f is the perturbing function and ε is the small perturbing parameter. Solutions to the system can then be shown to have the characteristic of returning to their initial position if one angular coordinate is incremented by an integer multiple of some characteristic angular period while the others are held fixed. This type of solution is defined as a torus, with characteristic frequencies defined by the constant rates of change of the angular coordinates.

Previous work by Wiesel has shown that an Earth-orbiting satellites' orbit can be described as a three-dimensional torus in six-dimensional phase space [1]. This is possible by expressing the satellite's position in the Earth-Centered-Earth-Fixed (ECEF) reference frame. In this frame, the satellite position vector is dependent on three periodic terms which can be used as approximations to the three characteristic frequencies of the torus, ω_i:

$$\begin{aligned}\omega_1 = \dot{M} &\approx \sqrt{\frac{\mu}{a^3}}\left[1 - \frac{3J_2R_\oplus^2}{2a^2(1-e^2)^{1.5}}\left(\frac{3}{2}sin^2(i) - 1\right)\right] \\ \omega_2 = \dot{\Omega} - \omega_\oplus &\approx -\frac{3\sqrt{\mu}J_2R_\oplus^2}{2a^{3.5}(1-e^2)^2}\cos(i) - \omega_\oplus \\ \omega_3 = \dot{\omega} &\approx \frac{3\sqrt{\mu}J_2R_\oplus^2}{2a^{3.5}(1-e^2)^2}\left(\frac{5}{2}sin^2(i) - 1\right)\end{aligned} \tag{2}$$

Where $\omega_\oplus$ and $R_\oplus$ are the rotational rate and radius of the Earth respectively, J_2 is the dominant coefficient in the geopotential, μ is the gravitational parameter and M, Ω, ω, a, e and i are the familiar classical orbital elements. These frequencies can then be used to form the action-angle variables for the system. Specifically, the angular coordinates are the integrals of the three frequencies and are all linear with time - M, $\Omega - \omega_\oplus t$, and ω - while the conjugate momenta can be calculated using the principle of least action and have been shown to be approximately equal to the Delaunay momenta [2]. Using these action-angle variables, the approximate Hamiltonian can be written as

$$K = -\frac{\mu^2}{2P_1^2} - \omega_\oplus + \frac{\mu^4 J_2 R_\oplus^2 (P_3^2 - 3P_2^2)}{4P_1^3 P_3^5} \tag{3}$$

Where P_i are the Delaunay momenta.

The method of producing a torus capable of accurately modeling a satellite's orbit has been developed and reported on previously by Wiesel [1][2] and can be broken into 3 steps:

1.) Numerically integrate the orbit to produce a dense set of position vector data in the ECEF frame
2.) Identify the orbit's fundamental frequencies (the torus basis frequencies) to a high degree of accuracy using a modified Laskar frequency algorithm
3.) Write each physical coordinate (x,y,z) as a Fourier series in the three torus basis frequencies

This method has been shown by Bordner to predict a satellite's position to an accuracy of tens of meters over a period of six months for certain types of orbits [3]. Other research by Derbis and Little has demonstrated limitations of the method in that it cannot readily accommodate non-conservative forces such as air drag or perturbations due to station-keeping maneuvers on operational satellites [4][5].

The current work builds on the torus construction method described above by using observational data in the form of TLEs to identify the torus basis frequencies and adding a second-order component to the torus coordinates to account for air-drag.

3. METHOD

For the current effort, four test objects were chosen from the satellite catalog based on the criteria that they were uncontrolled satellites in LEO orbiting above 300km such that air drag effects would be minimal. Tab. 1 gives general information on the approximate orbits of each test object.

Tab. 1. Orbital information for test satellites

Name	Catalog #	Launch Date	Period [min]	Inclination [deg]	Apogee [km]	Perigee [km]	Eccentricity
Hubble Space Telescope	20580	4/24/1990	95.93	28.47	566	561	3.836E-04
Thor Ablestar Rocket Body	59	10/4/1960	106.44	28.25	1203	921	1.893E-02
Delta 1 Rocket Body #1	341	7/10/1962	157.52	44.77	5619	949	2.414E-01
Delta 1 Rocket Body #2	8133	8/27/1975	95.21	25.30	700	357	2.753E-02

Approximately 18 months of TLE data was collected for each test subject from the website http://celestrak.com. M, Ω, and ω data was extracted in order to determine the torus basis frequencies. This was done by plotting the data vs time and fitting second-order polynomials to the data using a least squares technique. The curve fits, and the residuals from those fits for the Thor Rocket Body can be seen in Fig. 2. The first-order coefficients from these curve-fits are the desired torus basis frequencies.

Starting from an initial position and velocity derived from the initial TLE in the data set and SGP4 algorithms, each test subject's orbit was numerically integrated for a total of one year's time. The numerical integrator used takes into account the first twenty terms in the Earth's geopotential from the EGM96 model. Error checking was accomplished by calculating the Hamiltonian given in Eq. 3 at each time step and ensuring its value stayed constant. For all cases, error in the Hamiltonian did not exceed 10^{-13}.

The numerical data was then analyzed to identify the orbit's fundamental frequencies using the modified Laskar frequency algorithm developed and applied previously by Wiesel and Bordner [1][3]. Fig. 1 shows the partial frequency spectrum of the Thor Rocket Body orbit and identifies the major peaks near integer multiples of the Mean anomaly frequency (ω_1 and $2\omega_1$).

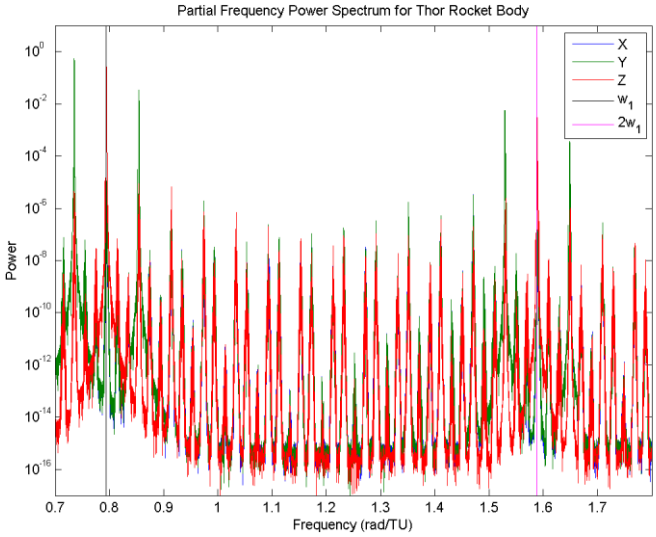

Fig. 1. Partial frequency spectrum for the Thor Rocket Body

Having identified the fundamental frequencies of the numerically integrated orbit, the numerical data was fit to a Fourier series in the three basis frequencies. This Fourier series expresses physical coordinates in terms of torus coordinates and is of the form

$$\vec{q} = \sum_{\vec{j}} \left(C_{\vec{j}} cos\vec{j} \cdot \vec{Q} + S_{\vec{j}} sin\vec{j} \cdot \vec{Q} \right) \tag{4}$$

Where $\vec{q}$ is a vector containing physical, Cartesian coordinates, $\vec{j}$ is a vector summation index with each vector corresponding to a linear combination of the three basis frequencies identifying a peak in the power spectral density function plot of the numerically integrated trajectory, C and S are matrices of Fourier coefficients and $\vec{Q}$ is a vector containing torus coordinates.

The initial torus basis frequencies were then compared to the desired torus basis frequencies obtained from the TLEs. Following the initial torus construction, the differences between the two sets of frequencies were not negligible. In order to correct this difference, a frequency matching iteration was performed. This iteration was accomplished by calculating the change in initial conditions (position and velocity) that would give the desired change in basis frequencies. For this work, it was assumed that the initial position derived from the initial TLE in

the data set and SGP4 algorithms was accurate, and therefore held fixed, while the initial velocity was allowed to change. The reference (first-iteration) torus basis frequencies are grouped into a vector, $\vec{\omega}$, while the desired torus basis frequencies from the TLE data are grouped into $\vec{\omega}_0$. The frequency error can then be written as

$$\Delta\vec{\omega} = \vec{\omega} - \vec{\omega}_0 = \frac{\partial\vec{\omega}}{\partial\vec{P}}\Delta\vec{P} \tag{5}$$

Where $\vec{P}$ is the vector of the reference torus momenta and $\Delta\vec{P}$ is the unknown momentum offset between the reference and desired torus. Eq. 5 can be solved for $\Delta\vec{P}$ which yields

$$\Delta\vec{P} = \frac{\partial\vec{\omega}}{\partial\vec{P}}^{-1}\Delta\vec{\omega} \tag{6}$$

The Jacobian, $\partial\vec{\omega}/\partial\vec{P}$ can be found analytically in terms of the classical orbital elements by taking the torus momenta to be the DeLaunay momenta and writing the torus frequencies as partial derivatives of the system Hamiltonian, *K,* given previously in Eq. 3:

$$\vec{\omega} = \frac{\partial K}{\partial\vec{P}} \tag{7}$$

Therefore, the Jacobian can be written

$$\frac{\partial\vec{\omega}}{\partial\vec{P}} = \frac{\partial^2 K}{\partial\vec{P}^2} \tag{8}$$

In this way, a known offset in torus basis frequencies can be expressed as an offsets in the torus momenta.

In order to form the new torus with the correct basis frequencies (those derived from the TLEs), a new numerical integration must be carried out starting from some new initial position and velocity conditions. Therefore, the offset in torus momenta must be expressed as a change in the physical position and/or velocity. For this effort, as noted earlier, the initial position was held fixed while the initial velocity was allowed to change.

Let the physical and torus state vectors be

$$\begin{aligned}\vec{X} &= [\vec{r}^T\ \vec{v}^T]^T = \left[x\ y\ z\ v_x\ v_y\ v_z\right]^T \\ \vec{Y} &= \left[\vec{Q}^T\ \vec{P}^T\right]^T = [M\ \Omega\ \omega\ P_1\ P_2\ P_3]^T\end{aligned} \tag{9}$$

Then, the change in the physical state vector can be written in terms of a change in the torus state vector as

$$\Delta\vec{X} = \begin{bmatrix}\Delta\vec{r} \\ \Delta\vec{v}\end{bmatrix} = \frac{\partial\vec{X}}{\partial\vec{Y}}\Delta\vec{Y} \tag{10}$$

Where $\Delta\vec{Y} = \left[\Delta\vec{Q}^T \quad \Delta\vec{P}^T\right]^T$. The Jacobian $\partial\vec{X}/\partial\vec{Y}$ can be found analytically as

$$\frac{\partial\vec{X}}{\partial\vec{Y}} = \left(\frac{\partial\vec{Y}}{\partial\vec{Z}}\frac{\partial\vec{Z}}{\partial\vec{X}}\right)^{-1} \tag{11}$$

where

$$\vec{Z} = [M\ \Omega\ \omega\ a\ e\ i]^T \tag{12}$$

Is a vector containing the COEs. For a detailed derivation of the content of $\partial\vec{X}/\partial\vec{Y}$ see [6]. Then, setting the change in initial position, $\Delta\vec{r} = 0$, Eq. 10 can be re-written as two linear equations

$$\Delta\vec{r} = \vec{0} = A\Delta\vec{Q} + B\Delta\vec{P} \tag{13}$$

$$\Delta\vec{v} = C\Delta\vec{Q} + D\Delta\vec{P} \tag{14}$$

Where A, B, C and D are quadrants of $\partial\vec{X}/\partial\vec{Y}$:

$$\frac{\partial\vec{X}}{\partial\vec{Y}} = \begin{bmatrix} A & B \\ C & D \end{bmatrix} \tag{15}$$

Given $\Delta\vec{P}$ from Eq. 6, the change in initial velocity needed to give a desired change in torus basis frequencies can be found by first solving Eq. 13 for $\Delta\vec{Q}$ and substituting into Eq. 14 which gives

$$\Delta\vec{v} = (-CA^{-1}B + D)\Delta\vec{P} \tag{16}$$

Having now obtained a new initial physical state, $\vec{X}_0$, the torus construction process, starting with a new numerical integration, can be repeated to find a new torus with updated basis frequencies. This algorithm was repeated until the maximum basis frequency error was down to 10^{-12} rad/TU. With an updated torus with basis frequencies matching those obtained from the TLE curve fits, the satellite's physical position was extracted using the torus Fourier series of Eq. 4 and expressing the torus coordinates as the quadratic functions of time found in the TLE curve fits.

4. RESULTS

The process described above was attempted for each of the four test cases from Tab. 1. For both Delta Rocket Bodies, curves were fit to the TLE data set, however the residuals between the data and the curve fits for Mean anomaly were as high was 2 radians for Delta Rocket Body #2 and as high as 30 radians for Delta Rocket Body #1. For Delta Rocket Body #1, the authors believe the poor fit is a result of the way TLE data is formatted. Specifically, both revolution number and epoch time are based off of ascending node crossing. This can lead to errors in the revolution number count if the satellite is off slightly from the ascending node. For Delta Rocket Body #2, the poor fit is believed to be due to the relatively low orbit (perigee at 357 km), the approximately 350 km difference between perigee and apogee, and the high area-to-mass ratio of an empty rocket body resulting in significant air drag effects that vary widely throughout the orbit.

The Hubble Space Telescope (HST) is in a nearly circular orbit with an eccentricity of approximately 0.0004 at an altitude of approximately 560 km. It was expected then that the air drag effects experienced by the HST would be less pronounced and nearly uniform throughout the orbit. This was the case, as this time, the curve-fits left maximum residuals of only approximately 0.1 rad. With good curve-fits, and therefore reliable basis frequencies, the torus construction process was attempted, however the algorithm to identify the basis frequencies of the numerically integrated trajectory failed to correctly identify the smallest basis frequency, ω_3. The authors believe the cause of this difficulty to be the low eccentricity of the HST's orbit. In the torus construction algorithm, small eccentricities lead to singularities, similar to those encountered with classical perturbation theory. This problem has been encountered in earlier research by Bordner [3].

The Thor Rocket Body test case had a much larger eccentricity than the HST (0.02) and was at a higher altitude than the Delta Rocket Bodies. As a result, the problems in curve-fitting and torus construction seen in the previous cases were not encountered. Fig. 2 shows the curve fits for the Thor Rocket Body; this time, maximum residuals were on the order of 10^{-3} rad. From these curve fits, desired torus Basis frequencies were determined and are shown in Tab. 2.

Tab. 2. Thor Rocket Body desired torus basis frequencies

ω1 [rad/TU]	ω2 [rad/TU]	ω3 [rad/TU]
7.93727220765370E-01	-5.96705921687582E-02	1.36750321345160E-03

A total of four iterations of the frequency matching algorithm were necessary to match the torus basis frequencies to within the desired tolerance. Tab. 3 shows the progression of torus frequencies along with the residuals, calculated from the desired TLE curve-fit frequencies, and Tab. 4 shows the initial velocity changes made in each iteration of the frequency matching process. The magnitude of the total velocity change was approximately 0.25 percent of the initial velocity magnitude obtained from the TLEs and SGP4.

Tab. 3. Torus frequency matching for Thor Rocket Body

	ω1 [rad/TU]	ω2 [rad/TU]	ω3 [rad/TU]
Initial Torus	7.93732038441640E-01	-5.96704909422124E-02	1.36749993586527E-03
Iteration 1 Torus	7.93718780146312E-01	-5.96705786750190E-02	1.36747666904746E-03
Iteration 2 Torus	7.93727192361304E-01	-5.96705924650170E-02	1.36750386446849E-03
Iteration 3 Torus	7.93727221037809E-01	-5.96705921734135E-02	1.36750322508483E-03
Iteration 4 Torus	7.93727220771728E-01	-5.96705921687751E-02	1.36750321348700E-03
	ω1 residual [rad/TU]	**ω2 residual [rad/TU]**	**ω3 residual [rad/TU]**
Iteration 1 Torus	8.44061905791449E-06	-1.34937392023970E-08	2.65444041400165E-08
Iteration 2 Torus	2.84040659881413E-08	2.96258795273729E-10	-6.51016889919101E-10
Iteration 3 Torus	-2.72439071302699E-10	4.65529698123746E-12	-1.16332299696098E-11
Iteration 4 Torus	-6.35802521742335E-12	1.68962066560141E-14	-3.53998514529552E-14

Tab. 4. Changes to initial velocity in Thor Rocket Body torus fitting process

	Vx [DU/TU]	Vy [DU/TU]	Vz [DU/TU]
Initial Velocity	-9.98015949328921E-02	-8.11259141324669E-01	4.39329318458694E-01
Iteration 1 ΔV	2.45940386540720E-03	-2.58556420032001E-04	8.51464239486448E-05
Iteration 2 ΔV	-1.09486652807646E-04	1.50534148714208E-05	-3.35944758461485E-06
Iteration 3 ΔV	3.85930049076970E-06	5.54734206659374E-07	1.45063141307529E-07
Iteration 4 ΔV	3.20433729724457E-08	5.37472590607683E-09	3.03779212051191E-09
Total ΔV	2.34602586873582E-03	2.42942896228060E-04	-8.19350772974792E-05

The final iteration with matched basis frequencies was then used to predict the satellite location, and this predicted location was compared with the location obtained using SGP4 algorithms at the epoch time of each TLE in the data set. The first comparison was done calculating the torus coordinates, Q_i, as linear functions of time; that is:

$$\vec{Q}_i = \omega_i t + \omega_{i0}$$

The results of this comparison can be seen in Fig. 3.

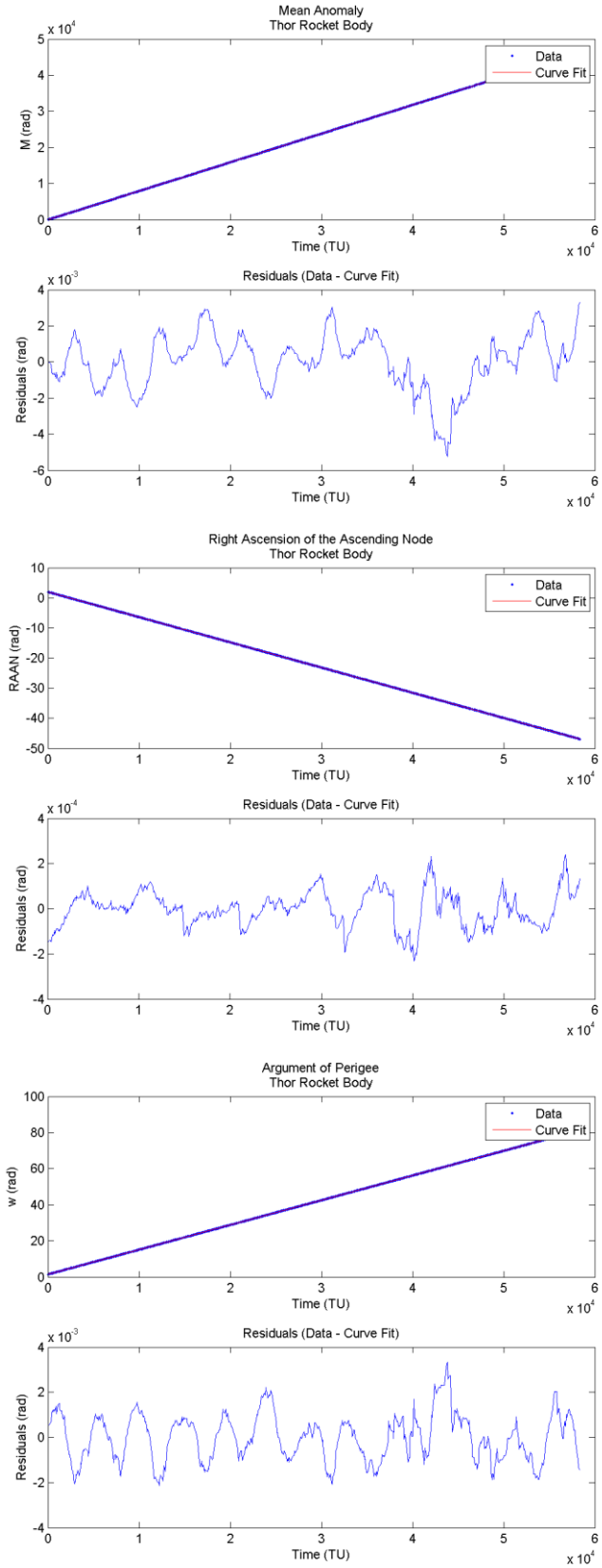

Fig. 2. TLE curve-fits for the Thor Rocket Body

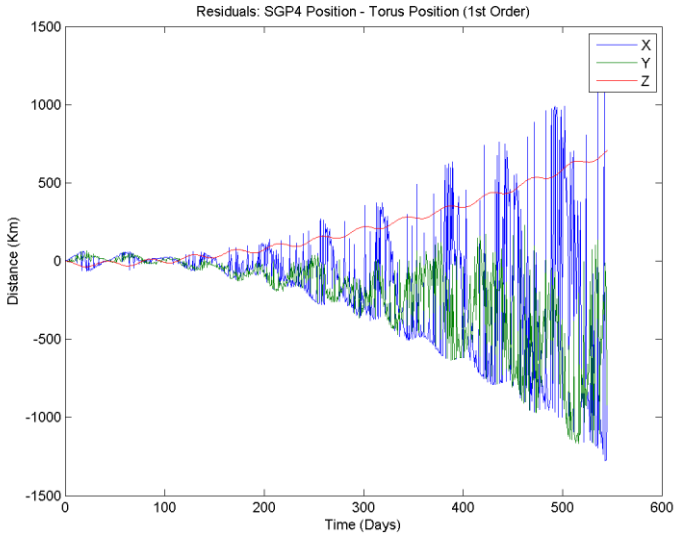

Fig. 3. Torus position error, calculated using first-order torus coordinates

It is evident that the torus in this configuration provides a poor position prediction with the position in error growing to a magnitude of nearly 1500km after 18 months. This, however, is expected as the TLE analysis showed that the torus coordinates increase as quadratic functions of time. To compensate for this, the torus coordinates were re-calculated, this time using the entire quadratic curve-fit at each time step. The results of this can be seen below in Figs. 4 and 5.

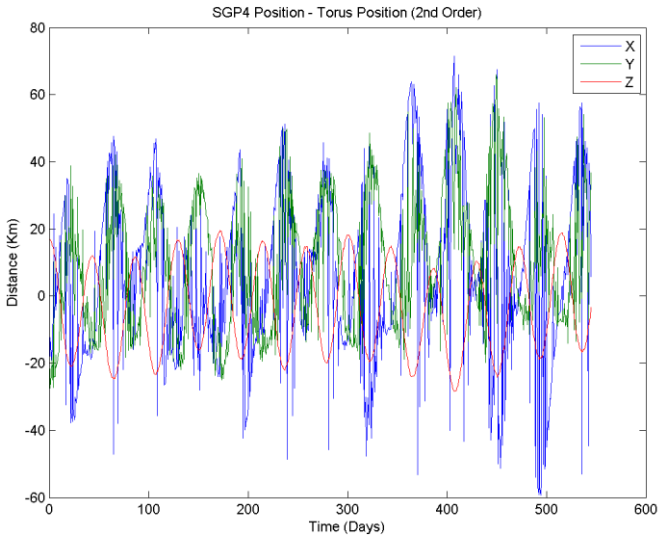

Fig. 4. Torus position error, calculated using second-order torus coordinates

These figures show that the maximum position error magnitude is now only approximately 78 km, and there is no apparent linear or quadratic growth in the error as was seen in the previous comparison (Fig. 3).

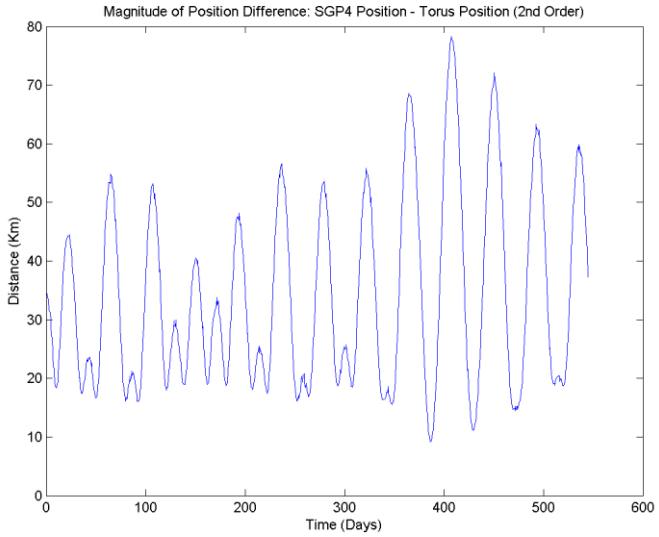

Fig. 5. Magnitude of torus position error, calculated using second-order torus coordinates

In order to further understand the causes of the remaining error in position prediction, a frequency analysis was done on the position error data. Figs. 6 and 7 show the results of this analysis and illustrate that the position error in all three physical coordinates oscillates predominately at the third torus basis frequency ω_3, and the X and Y coordinates have a secondary oscillation frequency equal to the second torus basis frequency, ω_2.

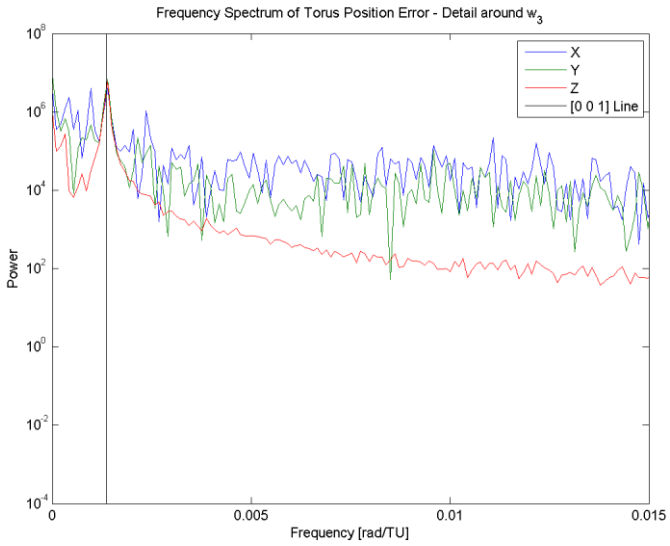

Fig. 6. Frequency spectrum of torus position error – ω_3 detail

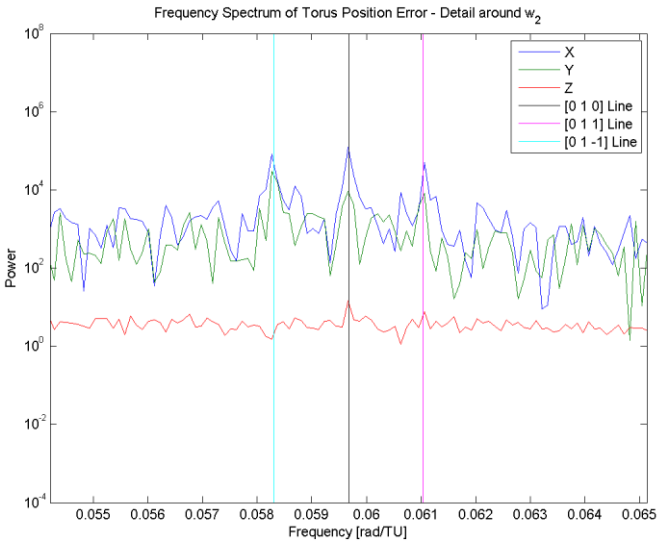

Fig. 7. Frequency spectrum of torus position error – ω_2 detail

5. CONCLUSIONS

The results discussed above show a number of promising results. First, the HST and Thor Rocket Body test cases show that it is possible to extract accurate KAM torus basis frequencies from observational data in the form of TLEs. Second, a method of making slight changes to torus basis frequencies was demonstrated by equating a desired change in basis frequencies to a small change in initial velocity. This capability allows the current torus construction method to be used in tandem with the TLE frequency identification routine to obtain a torus with the desired basis frequencies for a given satellite. The difficulties encountered with TLE curve fitting for the two Delta Rocket Bodies show that there may be limitations in the orbital regimes for which the current method of basis frequency extraction from TLEs can be useful; specifically, orbits in which air drag effects are moderate to minimal with little variation throughout the orbit.

It is the opinion of the authors that the residual position error seen in the Thor Rocket Body test case is due to two sources. First, the frequency analysis of the error discussed above shows that the torus construction method may not be adequately characterizing the contribution of the two smallest basis frequencies to the satellite's position. Second, perturbations from the Sun and Moon are currently not included in the torus model. These perturbations are masked in SGP4 and the TLEs due to frequent updates. Current research is being done by Wiesel to address both of these sources of error by further refining the torus construction algorithms to more accurately model the effects of ω_2 and ω_3 and by incorporating Solar and Lunar effects into the model.

6. REFERENCES

1. Wiesel, William E. "Earth Satellite Orbits as KAM Tori", *The Journal of the Astronautical Sciences*, *56*(2):151-162 (2008).

2. Wiesel, William E. "Earth Satellite Perturbation Theories as Approximate KAM Tori", *American Astronomical Society*, *10*(122) (2010).

3. Bordner, Ralph E. *Orbital Tori Construction Using Trajectory Following Spectral Methods.* PhD dissertation, Air Force Institute of Technology, 2010.

4. Derbis, Rachael M. *Modeling GPS Satellite Orbits Using KAM Tori.* MS thesis, Air Force Institute of Technology, 2008.

5. Little, Bryan D. *Application of KAM Theorem to Earth Orbiting Satellites.* MS thesis, Air Force Institute of Technology, 2009.

6. Wiesel, William E. "Motion Near an Earth Satellite KAM Torus." Unpublished Working Document.